行政院國家科學委員會專題研究計畫 成果報告

靜電驅動式微泵浦之動態特性研究分析
研究成果報告(精簡版)

計 畫 類 別 ： 個別型
計 畫 編 號 ： NSC 99-2218-E-167-002-
執 行 期 間 ： 99 年 09 月 01 日至 100 年 07 月 31 日
執 行 單 位 ： 國立勤益科技大學機械工程系

計 畫 主 持 人 ： 劉晉嘉

計畫參與人員： 碩士班研究生-兼任助理人員：李瑞河
博士班研究生-兼任助理人員：湯祥雯

處 理 方 式 ： 本計畫可公開查詢

中 華 民 國 100 年 09 月 07 日

The Study of Dynamic Analysis of the Electrostatic-Actuating Micro Pump

Chin-Chia Liu

[1] Department of Industrial Education and Technology, National Changhua University of Education, Bao-Shan Campus: Number 2, Shi-Da Road, Changhua, 500, Taiwan, R.O.C.

Email Address: ccliu@cc.ncue.edu.tw
Email Address: albertliu06@yahoo.com.tw

Abstract

Micro-electro-mechanical systems is that the size of component or the movement range is within micro grade, also called the Micromechanical or Microsystems. It is a cross-curricular research field, covering topics such as physics, optics, mechanics, electricity, biology and chemistry. The micro fluid system is an important branch of micro-electro-mechanical systems, it can be widely applied to fields such as medical, chemical analysis and lubricating, etc.. The micro pump is the actuating component of the micro fluid system.

The analytical modeling of the micro circular plate devices by electrostatic is problematic due to the complexity of the interactions between the electrostatic coupling effect, residual stress and the nonlinear electrostatic force. Therefore, the dynamic behavior of the micro circular plates is not easily analyzed using traditional analytic methods. Accordingly, this study develops an efficient computational scheme in which the nonlinear governing equation of the coupled electrostatic force acting, residual stress and hydrostatic pressure acting on the micro circular plates system is solved using a hybrid method (H.M.) which differential transformation with finite difference approximation method. In addition, this study shows the dynamic behavior of the micro circular plates by a DC actuating load.

Keywords: Pull-in voltage; Micro circular plate; Electrostatic actuator; Hybrid Method; Differential Transformation.

1 Introduction

In recent years, micro-electro-mechanical systems (MEMS) devices have been widely applied for a diverse range of applications, ranging from accelerometer and pressure sensors in automotive security systems [1], to micro-scale actuators in the aerospace and medical fields [2], electrostatic rotary comb actuators for micromirrors [3], actuators for Digital Micromirror Devices (DMDs) [4], and so forth. Therefore, MEM is highly worth to research for industry. The actuation systems used in today's MEMS devices can be broadly classified as either electrostatic [5], thermal, piezoelectric [6] or electromagnetic [7]. Of these various techniques, electrostatic actuation schemes are commonly preferred since they are easily fabricated using established surface micromachining techniques, have a rapid response and a low power consumption. In practice, the actuation effect in such schemes is created by generating an electrostatic force between the stationary and the moving parts of the actuator through the application of an external voltage. However, in implementing such a system, great care must be taken to specify appropriate values of the device parameters and operating conditions in order to prevent the so-called "pull-in phenomenon", in which the attractive electrostatic force induced by the external voltage exceeds the restoring force developed within the deflected membrane and causes it to collapse and make a momentary contact with the lower electrode. The voltage at which this phenomenon takes place is referred to as the "pull-in voltage" and is of critical importance in the design of many MEMs-based devices [8]. Generally speaking, the dynamic behavior of the micro circular plates used in MEMS electrostatic actuators is not easily analyzed using traditional methods such as Galerkin method due to the complexity of the interactions between the electrostatic coupling effects.

Differential transformation theory was originally proposed by Zhao in 1986 as a means of solving linear and nonlinear initial value problems in the circuit analysis domain. However, in more recent years, researchers have extended its use to the analysis of a variety of initial value problems in the mechanical engineering field [9-10]. Chen *et al.* [11] demonstrated that the hybrid method (H.M.) which differential transformation and finite difference method provides a precise and computationally-efficient means of analyzing the nonlinear dynamic behavior of fixed-fixed micro-beams. The same group also used the hybrid method to analyze the nonlinear dynamic response of an electrostatically-actuated micro circular plate subject to the effects of residual stress and a uniform hydrostatic pressure acting on the upper surface [12]. Finally, Kuo and Chen [13] employed the hybrid method (H.M.) which differential transformation and finite difference method to solve the nonlinear Burgers' equation for various values of the Reynolds number, including high values.

In the current study, the hybrid method (H.M.) is employed to analyze the electrostatic gap, membrane thickness, membrane radius of the dynamic behavior of the micro circular plates by a DC actuating load. In formulating the nonlinear governing equation of the circular plate, explicit account is taken of both the hydrostatic pressure and the residual stress. The hybrid method can be applied easily and efficiently for nonlinear electrostatic behavior to obtain numerical results of the micro circular plate.

2 Differential Transformation Theory

This section reviews the basic principles of differential transformation theory. Assume that $y(t)$ is an analytic function in the time domain *T*. The differential transformation of y at time $t = t_0$ in the K domain is given by

$$Y(k;t_0) = W(k)\left(\frac{d^k}{dt^k}(s(t)y(t))\right)_{t=t_0} \quad , \quad k \in K \,, \tag{2.1}$$

where k belongs to a set of non-negative integers which collectively define the K domain; $W(k)$ is a weighting factor; and $s(t)$ is a kernel function corresponding to $y(t)$. Note that $W(k)$ and $s(t)$ are both non-zero and $s(t)$ is analytic in the time domain. The inverse differential transformation of $Y(k;t_0)$ is formulated as

$$y(t) = \frac{1}{s(t)}\sum_{k=0}^{\infty}\frac{(t-t_0)^k}{k!}\frac{Y(k;t_0)}{W(k)} \quad , \quad t \in T \,, \tag{2.2}$$

in which $W(k) = H^k / k!$ and $s(t) = 1$. Note that H is the time interval.

At time $t_0 = 0$, Eq. (2.1) becomes

$$Y(k)=\frac{H^k}{k!}\left[\frac{d^k y(t)}{dt^k}\right]_{t=0} \quad , \quad k\in K \ . \tag{2.3}$$

From Eq. (2.2), the inverse differential transformation of $Y(k)$ is obtained as

$$y(t)=\sum_{k=0}^{\infty}\left(\frac{t}{H}\right)^k Y(k) \quad , \quad t\in T \ . \tag{2.4}$$

Substituting Eq. (2.3) into Eq. (2.4) gives

$$y(t)=\sum_{k=0}^{\infty}\frac{t^k}{k!}\left[\frac{d^k y(t)}{dt^k}\right]_{t=0} \quad , \quad t\in T \ . \tag{2.5}$$

Eq. (2.5) has the form of a Taylor series expansion. Therefore, the basic operational properties of the differential transformation method (D.T.M) can be summarized as follows:

(a) Linearity operation

$$T[\alpha\, p(t)+\beta q(t)]=\alpha P(k)+\beta Q(k) \, , \tag{2.6}$$

where T denotes differential transformation and α and β are any real number.

(b) Convolution operation

$$T[p(t)q(t)]=P(k)\otimes Q(k)=\sum_{\ell=0}^{k}P(\ell)Q(k-\ell) \, ,$$

$$T[p^m(t)]=kP(0)P^m(k)=\sum_{\ell=1}^{k}\left[(m+1)\ell\right]P(\ell)P^m(k-\ell) \quad , \quad m\in N \, , \tag{2.7}$$

where $\otimes$ denotes convolution.

(c) Differential operation

$$T\left[\frac{d^n p(t)}{dt^n}\right]=\frac{(k+n)!}{k!H^n}P(k+n) \, , \tag{2.8}$$

where n is the order of differentiation

(d) Differential transformation of $\sin(t)$ and $\cos(t)$ functions

$$T\left[\sin(\alpha t+\beta)\right]=\frac{(\alpha H)^k}{k!}\sin\left(\frac{\pi k}{2}+\beta\right) \, ,$$

$$T\left[\cos(\alpha t+\beta)\right]=\frac{(\alpha H)^k}{k!}\cos\left(\frac{\pi k}{2}+\beta\right) \, , \tag{2.9}$$

where α and β are any real number. [8,11-12].

3 Modeling of Micro Circular Plate

In deriving the nonlinear governing equation of motion of the micro circular plate shown in Fig. 1, an assumption is made that the plate is subject to displacements and small strains and undergoes an axi-symmetric bending effect. The dynamic governing equation is normalized for analytical convenience and is then solved using the hybrid method (H.M.).

3.1 Nonlinear governing equation of micro circular plate

As shown in Fig. 1, the micro-actuator system considered in this study comprises a movable circular plate with a thickness b attached at its perimeter to a fixed rigid substrate. The gap between the two plates is filled with air and has an initial height of u. The application of an external voltage across the two electrodes creates an electrostatic attractive force which causes the micro circular plate to deflect in the downward direction toward the lower substrate. The displacement w of the circular plate is assumed to vary as a function of both the radial position r and the time t, i.e. $w = w(r,t)$ .Due to the small physical size of the MEMS actuator system shown in Fig.1, it is essential to take the effects of hydrostatic pressure and residual stress into account when modeling the pull-in phenomenon. It is supposed that the symmetry deflection of micro circular plate is irrelevant to polar coordinate θ . Thus, the dynamic governing equation should be rewritten as follows [12]:

$$\rho A\frac{\partial^2 w}{\partial t^2}+D\left(\frac{\partial^2}{\partial r^2}+\frac{1}{r}\frac{\partial}{\partial r}\right)\left(\frac{\partial^2 w}{\partial r^2}+\frac{1}{r}\frac{\partial w}{\partial r}\right)-F_r\left(\frac{\partial^2 w}{\partial r^2}+\frac{1}{r}\frac{\partial w}{\partial r}\right)=\frac{\varepsilon_0 V^2}{2(u-w)^2}+h_0\,, \tag{3.1}$$

where ρ is the density of the micro circular plate, F_r is the residual force, ε_0 is the permittivity of free space, V is the voltage between the upper and lower electrodes and h_0 is the hydrostatic pressure which acts on the upper surface of the plate. Furthermore, D is the flexural rigidity of the plate can be expressed as

$$D=\frac{Eb^3}{12(1-\upsilon^2)}\ , \tag{3.2}$$

where E , b and υ are the Young's modulus, thickness and Poisson ratio of the micro circular plate, respectively. The boundary conditions for Eq. (3.1) are as follows:

$$w(r,t)=\frac{\partial w(r,t)}{\partial r}=0,\quad \text{at}\quad r=0 \tag{3.3}$$

$$w(r,t)=\frac{\partial w(r,t)}{\partial r}=0,\quad \text{at}\quad r=\pm R \tag{3.4}$$

where R denotes the radius of the circular plate. Meanwhile, the initial conditions are given by:

$$w(r,0)=\frac{\partial w(r,0)}{\partial t}=0\,. \tag{3.5}$$

3.2 Normalized nonlinear governing equation of micro circular plate

For analytical convenience, the displacement term u in the governing equation is normalized with respect to the initial gap height between the plates, the radial position term r is normalized with respect to the plate radius, and the time term t is normalized with respect to the constant T_1, i.e.

$$w^*=\frac{w}{u}\ ,\ r^*=\frac{r}{R}\ ,\ \text{and}\ t^*=\frac{t}{T_1}\ , \tag{3.6}$$

where $T_1=\sqrt{\rho b R^4/D}$.

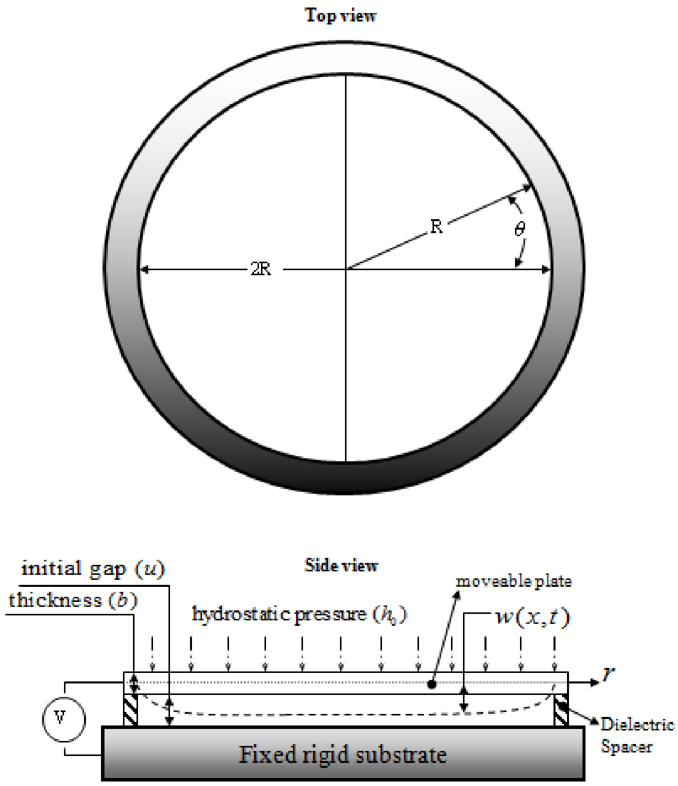

Figure 1: Schematic illustration of micro circular plate actuator system.

In addition, the voltage, residual stress and hydrostatic pressure terms are normalized as follows:

$$V^* = \sqrt{\frac{\varepsilon_0 R^4 V^2}{2Du^3}} \ , \quad F_r^* = \frac{F_r R^2}{D} \ , \quad \text{and } h_0^* = \frac{h_0 R^4}{Du} \ , \tag{3.7}$$

Substituting Eqs. (3.6) and (3.7) into Eqs. (3.1) and (3.4)~(3.6), the normalized governing equation can be expressed as follows:

$$\frac{\partial^2 w^*}{\partial t^{*2}} + \frac{\partial^4 w^*}{\partial r^{*4}} + \frac{2}{r^*}\frac{\partial^3 w^*}{\partial r^{*3}} - \frac{1}{r^{*2}}\frac{\partial^2 w^*}{\partial r^{*2}} + \frac{1}{r^{*3}}\frac{\partial w^*}{\partial r^*} - F_r^* \frac{\partial^2 w^*}{\partial r^{*2}} - F_r^* \frac{1}{r^*}\frac{\partial w^*}{\partial r^*} = \frac{V^{*2}}{(1-w^*)^2} + h_0^* \ , \tag{3.8}$$

The corresponding boundary conditions are given as

$$w^*(r^*,t^*) = \frac{\partial w^*(r^*,t^*)}{\partial r^*} = 0 , \quad \text{at} \quad r^* = 0$$

$$w^*(r^*,t^*) = \frac{\partial w^*(r^*,t^*)}{\partial r^*} = 0 , \quad \text{at} \quad r^* = 1 \tag{3.9}$$

The initial condition is given by

$$w^*(r^*,0) = \frac{\partial w^*(r^*,0)}{\partial t^*} = 0 \, . \tag{3.10}$$

The nonlinear electrostatic force term $V^{*2}/(1-w^*)^2$ in Eq. (3.8) can be approximated via the following Taylor expansion series:

$$\frac{V^{*2}}{(1-w^*)^2} = V^{*2}\left(1 + 2w^* + 3w^{*2} + 4w^{*3} + 5w^{*4} \cdots\cdots\cdots\right), \tag{3.11}$$

Neglecting the higher-order terms, and substituting Eq. (3.11) into Eq. (3.8), the nonlinear governing equation of the micro circular plate subject to the combined effects of electrostatic force, hydrostatic pressure and residual stress can be expressed as

$$\frac{\partial^2 w^*}{\partial t^{*2}}+\frac{\partial^4 w^*}{\partial r^{*4}}+\frac{2}{r^*}\frac{\partial^3 w^*}{\partial r^{*3}}-\frac{1}{r^{*2}}\frac{\partial^2 w^*}{\partial r^{*2}}+\frac{1}{r^{*3}}\frac{\partial w^*}{\partial r^*}-F_r^*\frac{\partial^2 w^*}{\partial r^{*2}}-F_r^*\frac{1}{r^*}\frac{\partial w^*}{\partial r^*} = V^{*2}\left(1+2w^*+3w^{*2}+4w^{*3}+5w^{*4}\right)+h_0^* \quad . \tag{3.12}$$

3.3 Application of H.M. to solution of nonlinear governing equation

In this section, the normalized governing equation given in Eq. (3.12), and the corresponding boundary conditions and initial condition given in Eqs. (3.9) and (3.10), respectively, are solved using the hybrid method (H.M.). The solution procedure commences by applying the differential transformation process with respect to the time domain t to each term in the governing equation, i.e.

$$T\left[\frac{\partial^2 w^*}{\partial t^{*2}}\right]=\frac{(k+1)(k+2)}{H^2}W(r^*,k+2)\,,$$

$$T\left[\frac{\partial^4 w^*}{\partial r^{*4}}\right]=\frac{d^4W(r^*,k)}{dr^{*4}}\,,$$

$$T\left[\frac{2}{r^*}\frac{\partial^3 w^*}{\partial r^{*3}}\right]=\frac{2}{r^*}\frac{d^3W(r^*,k)}{dr^{*3}}\,,$$

$$T\left[\frac{1}{r^{*2}}\frac{\partial^2 w^*}{\partial r^{*2}}\right]=\frac{1}{r^{*2}}\frac{d^2W(r^*,k)}{dr^{*2}}\,,$$

$$T\left[\frac{1}{r^{*3}}\frac{\partial w^*}{\partial r^*}\right]=\frac{1}{r^{*3}}\frac{dW(r^*,k)}{dr^*}\,,$$

$$T\left[F_r^*\frac{\partial^2 w^*}{\partial r^{*2}}\right]=F_r^*\frac{d^2W(r^*,k)}{dr^{*2}}\,,$$

$$T\left[F_r^*\frac{1}{r^*}\frac{\partial w^*}{\partial r^*}\right]=F_r^*\frac{1}{r^*}\frac{dW(r^*,k)}{dr^*}\,,$$

$$T\left[2V^{*2}w^{*2}\right]=2V^{*2}W(r^*,k)\,,$$

$$T\left[3V^{*2}w^{*2}\right]=3V^{*2}\left(W(r^*,k)\otimes W(r^*,k)\right)=3V^{*2}\left(\sum_{\ell=0}^{k}W(r^*,\ell)W(r^*,k-\ell)\right),$$

$$T\left[4V^{*2}w^{*3}\right]=4V^{*2}\left(\sum_{\ell=1}^{k}\left[(3+1)\ell-k\right]W(r^*,\ell)W^3(r^*,k-\ell)\right),$$

$$T\left[5V^{*2}w^{*4}\right]=5V^{*2}\left(\sum_{\ell=1}^{k}\left[(4+1)\ell-k\right]W(r^*,\ell)W^4(r^*,k-\ell)\right),$$

$$T\left[V^{*2}\right]=V^{*2}\delta(k)\,,$$

$$T\left[h_0^*\right]=h_0^*\delta(k)\,. \tag{3.13}$$

Note that $\delta(k)$ is specified as

$$\delta(k)=\begin{cases}1 & \text{for} \quad k=0\\ 0 & otherwise\end{cases}\,.$$

In the second stage of the solution procedure, the finite difference approximation method is applied with respect to r^* to the transformed versions of the equation of motion, boundary conditions and initial conditions, respectively. Applying the fourth-order accurate central difference scheme, which the equation can be expressed as follows:

$$\frac{(k+1)(k+2)}{H^2}W_i(k+2)+\frac{W_{i+2}(k)-4W_{i+1}(k)+6W_i(k)-4W_{i-1}(k)+W_{i-2}(k)}{\Delta r^{*4}}+\frac{1}{r^{*3}_{i}}\frac{W_{i+1}(k)-W_{i-1}(k)}{2\Delta r^*}$$
$$-\frac{1}{r^{*2}_{i}}\frac{W_{i+1}(k)-2W_i(k)+W_{i-1}(k)}{\Delta r^{*2}}+\frac{2}{r^*_i}\frac{W_{i+2}(k)-2W_{i+1}(k)+2W_{i-1}(k)-W_{i-2}(k)}{2\Delta r^{*3}}$$
$$-F_r^*\frac{W_{i+1}(k)-2W_i(k)+W_{i-1}(k)}{\Delta r^{*2}}-F_r^*\frac{1}{r^*_i}\frac{W_{i+1}(k)-W_{i-1}(k)}{2\Delta r^*}=V^{*2}\delta(k)+2V^{*2}W_i(k) \quad , \quad (3.14)$$
$$+3V^{*2}\left(\sum_{\ell=0}^{k}W_i(\ell)W_i(k-\ell)\right)+4V^{*2}\left(\sum_{\ell=1}^{k}\left[(3+1)\ell-k\right]W_i(\ell)W_i^3(k-\ell)\right)$$
$$+5V^{*2}\left(\sum_{\ell=1}^{k}\left[(4+1)\ell-k\right]W_i(\ell)W_i^4(k-\ell)\right)+h_0^*\delta(k)$$

where Δr^* is the radius interval and i is a position index in the r direction. In Eq. (3.14), $W_i(k+2)$ is the only unknown parameter.

4 Numerical Results and Discussion

In this study, the material and geometry parameters considered in the present analyses are summarized in Table 1. Figure 2 illustrates the variation of the micro plate deflection in the radial direction as a function of the applied voltage. The results show that at voltages lower than the pull-in voltage, the micro plate deflects symmetrically about its center point. As expected, the deflection of the micro plate increases with an increasing voltage. Furthermore, it is observed that the pull-in voltage has a theoretical value of 287.6 V for the micro plate parameters considered in Table 1.

Figure 3 shows the variation of the dimensionless center-point deflection with the applied voltage as a function of the initial gap between the two plates. The results indicate that the pull-in voltage increases as the initial gap is increased from 0.5 μm to 1.5 μm .

Figure 4 illustrates the variation of the pull-in voltage with the circular plate radius. In performing the analysis, the pull-in voltage reduces as the circular plate radius increases as the result of a loss in rigidity as the circular plate radius is increased. Finally, Figure 5 depicts the dependence of the pull-in voltage on the circular plate thickness. It is seen from figure 5 that the the circular plate thickness increases, pull-in voltage are increased due to an increase in the circular plate flexural rigidity.

Table 1. Material and geometry parameters of micro fixed-fixed beam model

Parameters	Value
Young's modulus (E) (GPa)	169
Poisson's Ratio (ν)	0.3
Density (ρ) (Kg/m^3)	2.33×10^3
Permittivity of free space (ε_0) (F/m)	8.8541878×10^{-12}
Thickness of the micro circular plate (b) (μm)	20
Initial gap (u) (μm)	1
Radius of the plate (R) (μm)	250

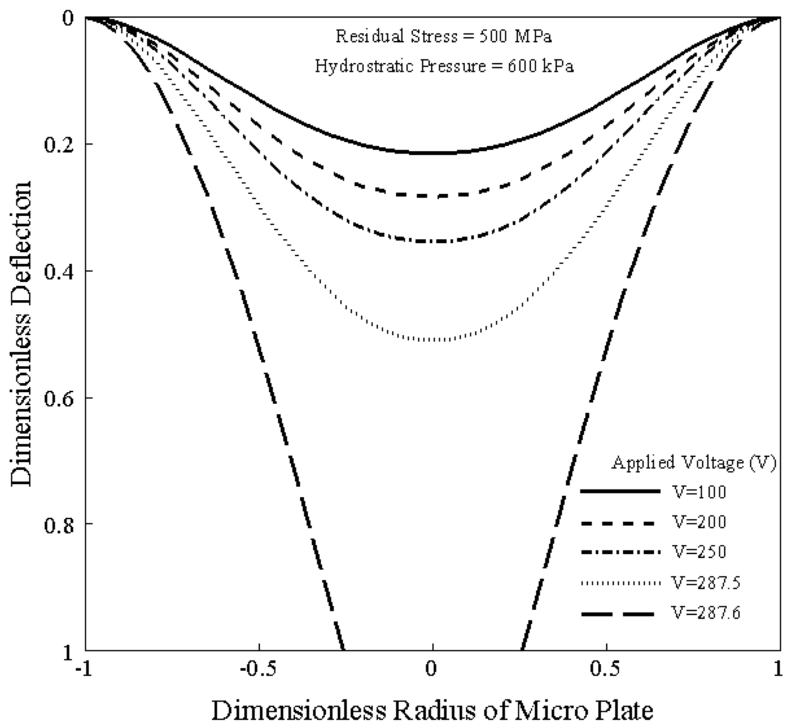

Fig. 2. Variation of dimensionless deflection with dimensionless radius of circular plate as function of applied voltage.

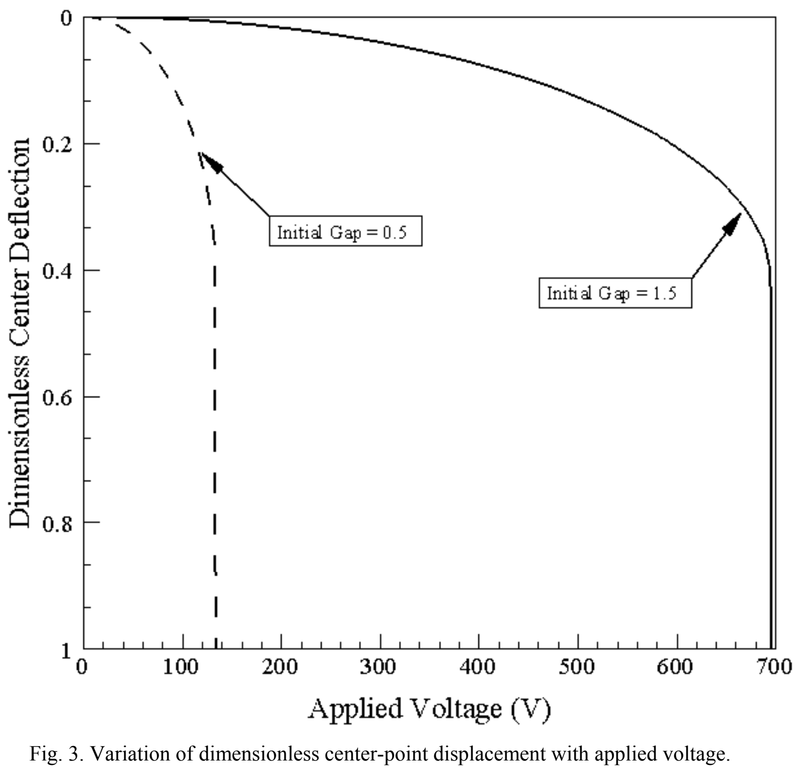

Fig. 3. Variation of dimensionless center-point displacement with applied voltage.

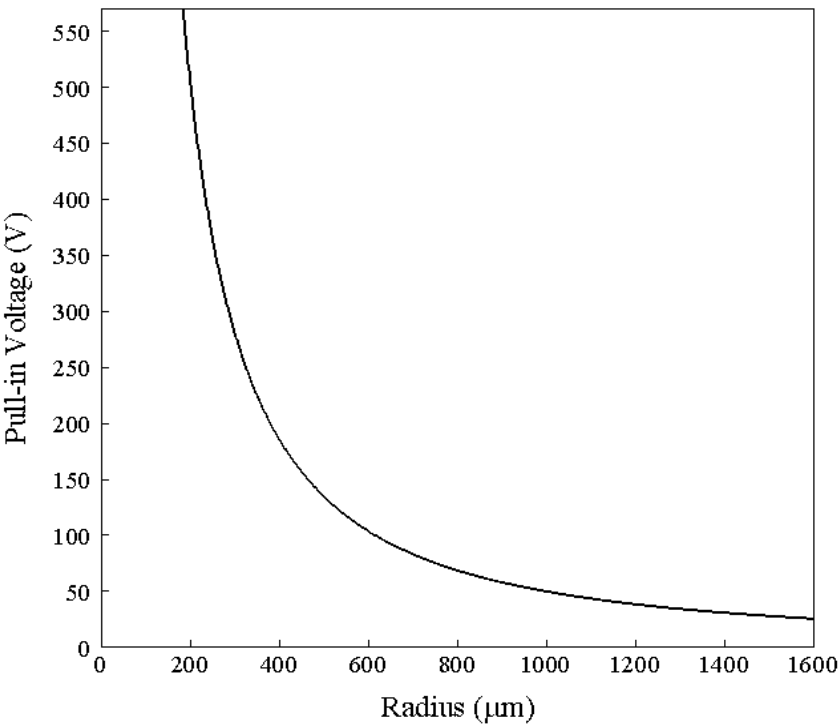

Fig. 4. Variation of pull-in voltage with radius of the micro circular plate.

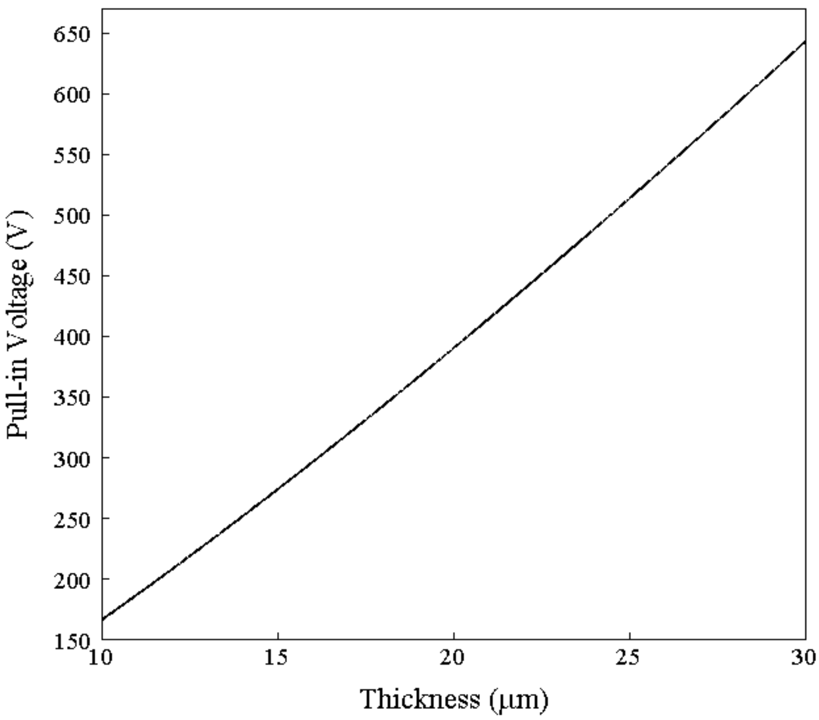

Fig. 5. Pull-in voltage versus micro-beam thickness

5 Conclusion

This study has applied a hybrid method (H.M.) scheme comprising the differential transformation method and the finite difference approximation technique to analyze the nonlinear dynamic response of the circular plate. In contrast to previous studies, the governing equation developed in this study takes into account the effects of both the hydrostatic force acting on the upper surface of the circular plate and the residual stress within the plate itself. In general, the present results have confirmed that the micro circular plate becomes structurally unstable at voltages equal to or greater than the pull-in voltage and collapses and makes contact with the lower electrode as a result. Furthermore, the results have shown that the magnitude of the pull-in voltage reduces as the circular plate radius increases due to a loss in structural rigidity. Overall, the results have confirmed that the proposed hybrid method scheme represents a computationally efficient of predicting the dynamic response of the micro circular plate commonly employed in electrostatically actuated MEMS-based devices.

Acknowledgements

The authors gratefully acknowledge the financial support provided to this study by the National Science Council of Taiwan under Grant Number NSC-99-2218-E-167-002.

References

[1] http://www.freescale.com/

[2] Son, I. S., Lal, A., Hubbard, B. and Olsen, T., A multifunctional silicon-based microscale surgical system. *Sensors and Actuators A*. Vol. 91, (2001), 351-356.

[3] Hu, M., Du, H., Ling, S., Liu, B., and Lau, G., Fabrication of a rotary micromirror for fiber-optic switching. *Microsyst Technol*. Vol. 11, (2005), 987–990.

[4] http://www.ti.com/

[5] Maluf, N.I., Reay, R.J., and Kovacs, G.T.A., High-Voltage devices and circuits fabricated using foundry CMOS for use with electrostatic MEM actuators. *Sensors and Actuators A*. Vol. 52, (1996), 187-192.

[6] Ghader, R., Ahmadali, T. and Mikhail Z., Application of piezoelectric layers in electrostatic MEM actuators: controlling of pull-in voltage. *Microsyst Technol*. Vol. 12, (2006), 1163–1170.

[7] Rajesh, L., Saniya, L., Jemmy, S. B., Yves, H. B. and Peter, J. H., Simulated and experimental dynamic response characterization of an electromagnetic microvalve. *Sensors and Actuators A*. Vol. 143, (2008), 399-408.

[8] Cha'o-Kuang Chen, Chin-Chia Liu, Hsin-Yi Lai, Nonlinear Dynamic Behavior Analysis of Micro Electrostatic Actuator based on a Continuous Model Under Electrostatic Loading. *ASME Journal of Applied Mechanics*. Vol. 78, (2011), 031003–1~031003–9.

[9] Chiou, J. S., and Tzeng, J. R., Application of the Taylor transform to nonlinear vibration problems. *ASME, J. of Vibration and Acoustics*. Vol. 118, (1996), 83-87.

[10] Chen, C. L., and Liu, Y. C., Solution of two -boundary-value problems using the differential transformation method. *Journal of optimization theory and application*. Vol. 99, (1998), 23-35.

[11] Chen, C. K., Lai, H. Y., and Liu, C. C., Application of hybrid differential transformation/finite difference method to nonlinear analysis of micro fixed-fixed beam. *Microsyst Technol*. 15, (2009), 813–820.

[12] Chen, C. K., Lai, H. Y., and Liu, C. C., Nonlinear Micro Circular Plate Analysis Using Hybrid Differential Transformation / Finite Difference Method. *CMES: Computer Modeling in Engineering & Sciences*. Vol. 40, No. 2, (2009), 155-174.

[13] Kuo, B. L., and Chen, C. K., Application of the Hybrid Method to the Solution of the Nonlinear Burgers' Equation. *ASME J. Appl. Mech.*. Vol. 70, (2003), 926–929.

國科會補助計畫衍生研發成果推廣資料表

日期:2011/09/02

國科會補助計畫	計畫名稱: 靜電驅動式微泵浦之動態特性研究分析
	計畫主持人: 劉晉嘉
	計畫編號: 99-2218-E-167-002- 學門領域: 結構與振動

無研發成果推廣資料

99 年度專題研究計畫研究成果彙整表

計畫主持人：劉晉嘉			計畫編號：99-2218-E-167-002-				
計畫名稱：靜電驅動式微泵浦之動態特性研究分析							
成果項目			量化			單位	備註（質化說明：如數個計畫共同成果、成果列為該期刊之封面故事...等）
			實際已達成數（被接受或已發表）	預期總達成數(含實際已達成數)	本計畫實際貢獻百分比		
國內	論文著作	期刊論文	0	0	100%	篇	
		研究報告/技術報告	0	0	100%		
		研討會論文	0	1	100%		
		專書	0	0	100%		
	專利	申請中件數	0	0	100%	件	
		已獲得件數	0	0	100%		
	技術移轉	件數	0	0	100%	件	
		權利金	0	0	100%	千元	
	參與計畫人力（本國籍）	碩士生	0	0	100%	人次	
		博士生	0	0	100%		
		博士後研究員	0	0	100%		
		專任助理	0	0	100%		
國外	論文著作	期刊論文	0	1	100%	篇	
		研究報告/技術報告	0	0	100%		
		研討會論文	0	0	100%		
		專書	0	0	100%	章/本	
	專利	申請中件數	0	0	100%	件	
		已獲得件數	0	0	100%		
	技術移轉	件數	0	0	100%	件	
		權利金	0	0	100%	千元	
	參與計畫人力（外國籍）	碩士生	0	1	100%	人次	
		博士生	0	1	100%		
		博士後研究員	0	0	100%		
		專任助理	0	0	100%		

其他成果 (無法以量化表達之成果如辦理學術活動、獲得獎項、重要國際合作、研究成果國際影響力及其他協助產業技術發展之具體效益事項等，請以文字敘述填列。)	無

	成果項目	量化	名稱或內容性質簡述
科教處計畫加填項目	測驗工具(含質性與量性)	0	
	課程/模組	0	
	電腦及網路系統或工具	0	
	教材	0	
	舉辦之活動/競賽	0	
	研討會/工作坊	0	
	電子報、網站	0	
	計畫成果推廣之參與（閱聽）人數	0	

國科會補助專題研究計畫成果報告自評表

請就研究內容與原計畫相符程度、達成預期目標情況、研究成果之學術或應用價值（簡要敘述成果所代表之意義、價值、影響或進一步發展之可能性）、是否適合在學術期刊發表或申請專利、主要發現或其他有關價值等，作一綜合評估。

1. 請就研究內容與原計畫相符程度、達成預期目標情況作一綜合評估

■達成目標

□未達成目標（請說明，以 100 字為限）

　　□實驗失敗

　　□因故實驗中斷

　　□其他原因

說明：

2. 研究成果在學術期刊發表或申請專利等情形：

論文：□已發表 ■未發表之文稿 □撰寫中 □無

專利：□已獲得 □申請中 ■無

技轉：□已技轉 □洽談中 ■無

其他：（以 100 字為限）

3. 請依學術成就、技術創新、社會影響等方面，評估研究成果之學術或應用價值（簡要敘述成果所代表之意義、價值、影響或進一步發展之可能性）（以 500 字為限）

意義：

微流體系統是微機電系統的一個重要分支，微泵浦作為微流體系統的動力元件，是微流體發展技術的重要指標。微泵浦可以廣泛應用於醫療、化學分析、微流體供給和控制、LED 冷卻系統等等，成為近年的熱門研究領域，早期的微泵浦研究主要集中在製造及結構設計，而對靜、動態的分析模擬研究較為欠缺，故也限制了微泵浦性能的提升。所以，期望透過此計畫的分析研究可以縮短微泵浦研發週期，提高微泵浦產品的可靠度。

價值與影響：

(a) 靜電驅動式微泵浦的工作過程中包含了結構、靜電及流體的耦合作用，若直接採用多能量的耦合方程式進行模擬，則將造成計算量太大而浪費時間；本計劃將利用混合法計算微泵浦的驅動電壓與泵膜變形和泵腔容積的變化關係及關鍵參數的動態特性分析，以提高模擬效率。

(b) 本計劃可提供給國內高科技製造業如半導體製程及醫療生技作為改進靜電驅動式微泵浦研發設計之參考。

(c) 本計劃之靜電驅動式微泵浦的研究成果，有助於微流體領域的後續發展。